Preliminary comparisons of thermal hydraulic characteristics of core using from 10 by 10 fuel assembly to 20 by 20 fuel assembly for SMART

Min-Gil Kim, Youho Lee, Jeong Ik Lee*
Dept. Nuclear & Quantum Eng., KAIST, 373-1, Guseong-dong, Yuseong-gu, Daejeon, 305-701, Republic of Korea
**Corresponding author: jeongiklee@kaist.ac.kr*

1. Introduction

Nowadays, development of small modular reactor (SMR) which can be manufactured in factory and constructed by adding module is came to the fore. The existing SMR designs are mostly based on the current PWR technology. This is also true for the nuclear fuel for SMR today, which most SMRs use rod type fuels based on the well accumulated experiences from commercial LWRs.

The reference reactor of this study is SMART, which is developed in Korea and it is originally designed to use rod-type fuel in 17 by 17 assembly. But, under SMR condition, adjusted fuel design can be more appropriate for changed thermal hydraulic conditions from large LWRs. In this preliminarily study, authors will discuss about the effects to thermal hydraulic variation occurred by assembly design change, from 10 by 10 assembly design to 20 by 20 assembly.

2. Fuel assembly design

Authors designed various fuel assemblies ranging from 10 by 10 to 20 by 20 while changing various geometry factors. Current SMART fuel assembly is 17 by 17. Table I and II show the design of SMART fuel rod and assembly[1].

Table I: Geometry of SMART Fuel rod[1]

Division	Length(mm)
Pellet Diameter	8.05
Gap Thickness	0.085
Cladding Thickness	0.64
Fuel Pitch	12.6
Fuel Active height	2000

Table II: SMART core design[1]

Division	
Total height	2400mm
Fuel rod #	264 per assembly
Fuel Assembly	17 by 17
Fuel assembly #	57
Core barrel diameter	2182mm

As a preliminary step to evaluate thermal hydraulic performances of each type under SMART operating condition, following assumptions were imposed to make a fair thermal hydraulic comparison of each assembly[1].

1. Overall power of cores should be the same.
2. Core has the same radial and axial peaking factors regardless of individual assembly design.
3. Core has the same cladding and gap thickness regardless of individual assembly design.
4. Core has the same moderator to fuel volume ratio regardless of individual assembly design.
5. Each assembly has same length and width with 17 by 17 reference fuel assembly.

Since total amount of cladding material in the core will change due to the aforementioned assumptions, authors calculated the total required change of enrichment of each core to maintain the same total mass of U-235 for each assembly. Fig.1 shows the diameters and pitches of each core. Fig.2 shows the amount of cladding material in single assembly and enrichment of each assembly which both are normalized with values from 17 by 17 reference assembly. As it can be seen from the both figures, the total enrichment of U-235 does not significantly increase due to the increase in the cladding material.

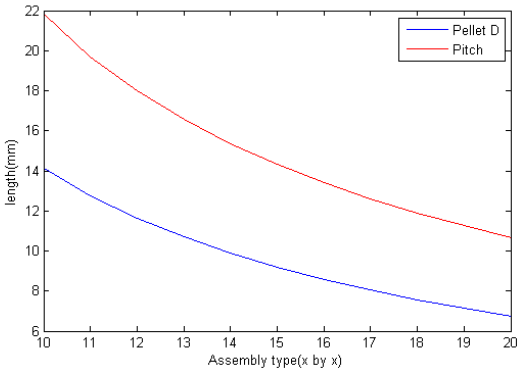

Fig.1. Fuel pellet diameter and pitch for each assembly

[1] Neutronic aspects of the two fuel types were not considered in this preliminary thermal hydraulic evaluation

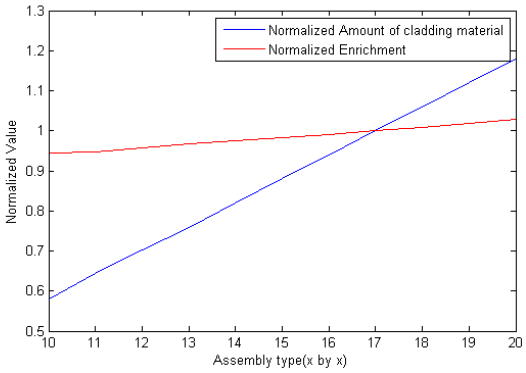

Fig.2. Normalized amount of cladding material and enrichment of fuel.

3. Comparison of Thermal Hydraulic Performances

In this section, we will compare thermal hydraulic performances of each core. Thermal hydraulic performances of each assembly are calculated by a code developed for this study, and the code is named as Reactor_TH, which is an in-house code developed by KAIST research team. Core pressure drop, minimal departure from nucleate boiling ratio (MDNBR), fuel centerline temperature and stored energy in fuel are the major factors for the comparison

3.1 Pressure Drop

While the coolant flows through a reactor core, there exists pressure drop due to the friction, sudden contraction, and expansion. Core pressure drop affects the pump requirement of the system or natural circulation characteristic of the primary loop. In this section, core pressure drop during the full power operation is compared.

Core pressure drop of rod-type fuel is calculated by the following steps. We assumed that two kinds of pressure drop in a rod-type fuel pressure drop exist, which are the grid spacer and friction pressure drop. Frictional pressure drop is calculated by Eq. (1) and Eq. (2). In laminar region, friction factor was determined by Eq. (1). For the turbulent region, Colbrook correlation was used. In the transition region, where the Reynolds number is between 2,000 and 3,000, friction factor was calculated by linear interpolation.

If Re<2000, $f = 64/\mathrm{Re}$ (1)

If Re>3000, $$\frac{1}{\sqrt{f}} = -2.0\log_{10}\left(\frac{\varepsilon/D}{3.7} + \frac{2.51}{\mathrm{Re}\sqrt{f}}\right) \quad (2)$$

Hydraulic diameter and heated diameter are calculated by following equations, Eq. (3).

$$D_{wetted} = D_{heated} = 4\times\frac{P^2 - (D/2)^2\times\pi}{\pi\times D} \quad (3)$$

After the calculation of the friction factor, pressure loss coefficient can be calculated by multiplying fuel total length and dividing into fuel hydraulic diameter.

Pressure loss coefficient of grid spacer was referred from KAERI's report [1]. Sum of the pressure loss coefficient is found to be 6.25. We assumed that pressure loss coefficient of grid spacer includes sudden contraction and sudden expansion effect.

Fig.3 shows the core pressure drop of each type assembly.

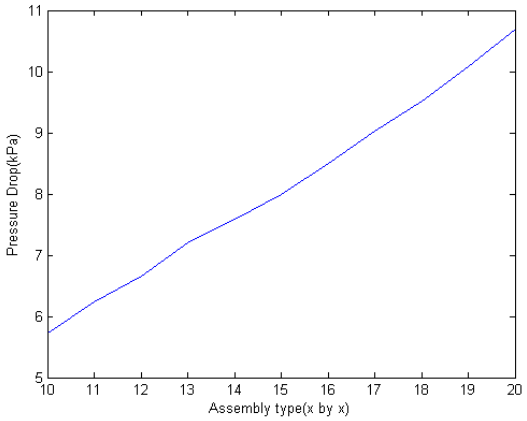

Fig.3. Core Pressure Drop of each assembly

3.2 MDNBR

MDNBR generally exists in the hot channel. Hence, we obtained the heat flux of a hot channel by multiplying peaking factors with the average fuel pin power. To evaluate the heat transfer coefficient, Collier's correlation is used for laminar flow, and Gnielinski's correlation is used for turbulent flow. These correlations were originally developed for a circular pipe. Eq. (4) shows the Collier's correlation [2], and Eq. (5) shows the Gnielinski's correlation [3]. Fig.4. shows Nusselt number change as a function of Reynolds number.

$$Nu = 0.17\,\mathrm{Re}^{0.33}\,\mathrm{Pr}^{0.43}\left[\frac{\mathrm{Pr}}{\mathrm{Pr}_W}\right]^{0.25} Gr^{0.1} \quad (4)$$

$$Nu_D = \frac{(f/8)(\mathrm{Re}_D + 1000)\,\mathrm{Pr}}{1 + 12.7(f/8)^{1/2}(\mathrm{Pr}^{2/3} - 1)},\ \text{for}\ 0.5 \le \mathrm{Pr} \le 2000,$$
$$3000 \le \mathrm{Re}_D \le 5\times10^6,\ \text{and}\ (L/D) \ge 10 \quad (5)$$

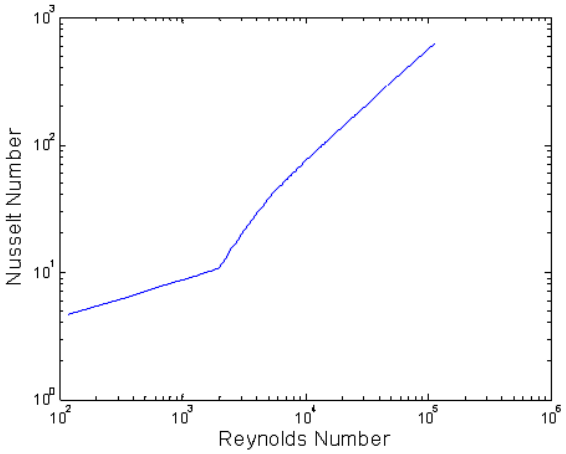

Fig. 4. Nusselt number for Reynolds number variation.

To calculate CHF, we used the CHF value from 2006 CHF Look-up Table [4]. This table is arranged by mass flux, pressure, and quality for 8mm circular tube. Diameter is replaced by hydraulic diameter. NIST property program is used for coolant property calculation. Power distribution is assumed to be a chopped cosine shape. Number of nodes is 20 for fuel radial direction, 5 for cladding radial direction, and 44 for axial direction.

Fig.5 shows the MDNBR of each type assembly.

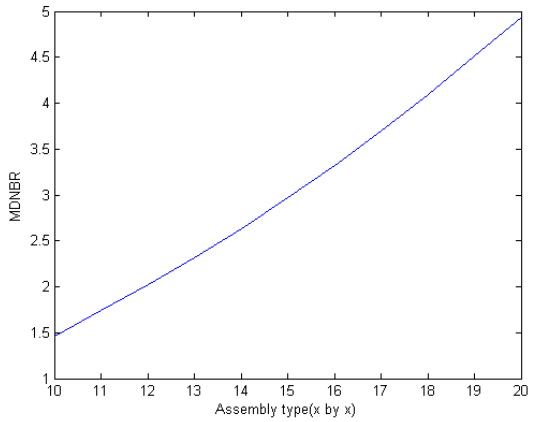

Fig.5. MDNBR of each assembly

3.3 Fuel Centerline Temperature

To check the safety of the fuel, fuel centerline temperature of hot fuel (in hot channel) should be calculated. If the temperature of cladding wall exceeds the saturation temperature of the coolant, then Jens-Lottes correlation is used for the cladding wall temperature calculation. Eq. (6) shows the Jens-Lottes correlation[5].

$$T_{wall} = T_{sat} + 60(q^{"} \times 10^{-6})^{0.25} \exp(-P/900) \qquad (6)$$

Gap is assumed to be an open gap. For the calculation of gap conductance, following Eq. (7) [6] is used.

$$q_g^{"} = h_g (T_{fo} - T_{ci})$$

$$h_g = \frac{k_{gas}}{\delta_{eff}} + \frac{\sigma}{\frac{1}{\varepsilon_f} + \frac{1}{\varepsilon_c} - 1} \frac{T_{fo}^4 - T_{ci}^4}{T_{fo} - T_{ci}}$$

$$k_{gas} = (k_1)^{x_1} (k_2)^{x_2}$$

$$k_{gas} = A \times 10^{-6} T^{0.79} W / cm^o K \qquad (7)$$

In this study, effective gap width is assumed to be the same with gap thickness. 96% helium and 4% argon fills the gap. The constant A in Eq. (7) is 15.8 for helium and 1.97 for argon. Since properties of fuel materials change with temperature, iterative calculations were conducted for the fuel centerline temperature analysis.

Fuel centerline temperature is obtained by solving conduction equation with finite-difference method, since thermal conductivity of the fuel changes with temperature. Coolant bulk temperature is calculated by Eq. (8).

$$H_z = H_{inlet} + \int_0^z q^{'}(z) dz \qquad (8)$$

Fig.6 shows the maximum fuel centerline temperature in the hot channel of each assembly.

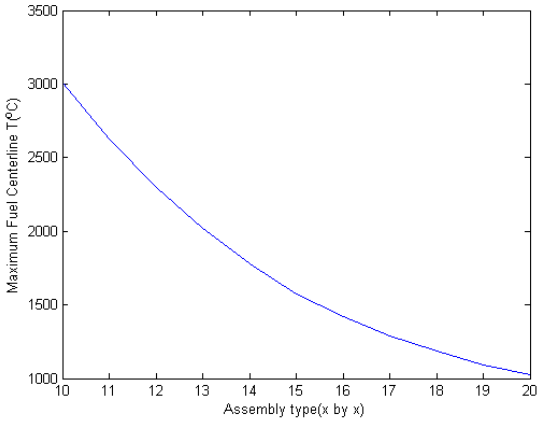

Fig.6. Maximum fuel centerline temperature of each assembly

3.4 Stored energy in Fuel

Authors compared stored energy in the whole fuel in reactor core. The reference point of the stored energy is at 300K. By using specific heat of UO_2, stored energy is calculated with the following equation, Eq. (9).

$$U = m \int_{300}^{T} C_p dT \qquad (9)$$

Fig.7 shows the stored energy of each assembly.

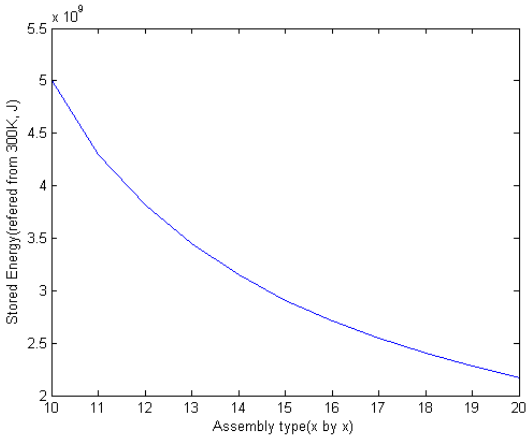

Fig.7 Stored Energy of each assembly

4. Summary and Conclusions

From the result of this study, safety margin is increased with increase of fuel rod number in assembly. Maximum fuel centerline temperature is decreased if the number of fuel rod per assembly increases, MDNBR is increased, and stored energy is decreased. However, the core pressure drop is increased when the number of fuel rodper assembly is increased but it is marginal. The total amount of cladding material is increased with the number of fuel rod per assembly but the increase in fuel enrichment to compensate this effect is also marginal. This issue is also important not only from the fuel enrichment perspective but also from the hydrogen generation point of view during a severe accident. Design studies considering the neutronic aspect and materials will be followed in the further study.

REFERENCES

[1] KAERI, “Basic Design Report of SMART”, KAERI/TR-2142/2002.
[2] J. G. Collier, Convective boiling and condensation, 2nd ed, Mcgraw-hill International Book Company(1981)
[3] V. Gnielinski, New equations for heat and mass transfer in turbulent pipe and channel flow, International Chemical Engineering, p.359–368(1976)
[4] D. C. Groeneveld, J. Q. Shan, et al., The 2006 CHF look-up table, Journal of Nuclear Engineering and Design, Vol. 237, 1909-1922(2007)
[5] W. H. Jens, and P. A. Lottes, Analysis of Heat Transfer, Burnout, pressure Drop and Density Data for High Pressure Water, ANL-4627, p.9,1951
[6] N. E. Todreas and M. S. Kazimi, Nuclear Systems I – Thermal Hydraulic Fundamentals, Taylor & Francis(1993)